

1 **Supplementary Information**

2

3 **Fe<sub>3</sub>O<sub>4</sub>@Zirconium Phosphate Core-shell Nanoparticles for pH-Sensitive and Magnetically**

4 **Guided Drug Delivery Application**

5 Himani Kalita<sup>a</sup>, Shashi Rajput<sup>b</sup>, B. N. Prashanth Kumar<sup>b</sup>, Mahitosh Mandal<sup>b</sup>, Amita Pathak<sup>a,\*</sup>

6

7 <sup>a</sup> Department of Chemistry, Indian Institute of Technology Kharagpur, West Bengal-721302,

8 India

9 <sup>b</sup> School of Medical Science and Technology, Indian Institute of Technology Kharagpur, West

10 Bengal-721302, India

11

12 \* Corresponding author:

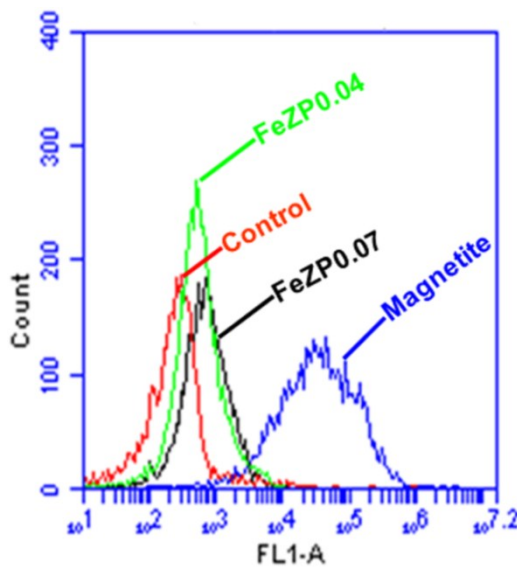
13 \*E-mail address: [ami@chem.iitkgp.ernet.in](mailto:ami@chem.iitkgp.ernet.in)

14 \*Tel.: +91-3222-283312, +91 94340 38730; Fax: +91-3222-282252

15

16 **1. Detection of ROS generation**

17 The intracellular generation of reactive oxygen species (ROS) from the prepared  
18 nanoparticles (viz. magnetite, FeZP0.07, and FeZP0.04) was measured using the oxidation  
19 sensitive dye 5-(and -6) chloromethyl-2',7'-dichlorodihydrofluorescein diacetate acetyl ester  
20 (CM-H<sub>2</sub>DCFDA). For the study, MDA-MB-231 cell lines were treated with the nanoparticles for  
21 24 h, after which the cells were trypsinized and suspended in PBS with CM-H<sub>2</sub>DCFDA  
22 (10  $\mu$ mol/L) for 1 h and subsequently washed with PBS to remove the unreacted dye. The  
23 samples were then acquired on the FL-1 channel of FACSCalibur (BD, Bioscience, USA) and  
24 analyzed using Cellquest software. For the analysis, untreated MDA-MB-231 cell lines were  
25 taken as the control. The generation of ROS from the nanoparticles was evaluated from the  
26 fluorescence measurement of the cell lines and the results are presented in Fig. S1. A dramatic  
27 ROS burst was observed in the cells treated with MNPs in contrast to the control, with profound  
28 peak shift annotating the intense fluorescence. On the contrary, insignificant peak shift was  
29 observed in the cells treated with FeZP0.04 inferring the production of ROS by the nanoparticles  
30 to be comparable with that in control cells. Further, FeZP0.07 treatments showed a slight shift of  
31 peak that indicates a small production of ROS by the nanoparticles in contrast to control cells.  
32 Thus, it can be inferred that MNPs elicits ROS production, which gets significantly reduced with  
33 the increase in thickness of zirconium phosphate shell on magnetite core in the core-shell  
34 nanoparticles.



35

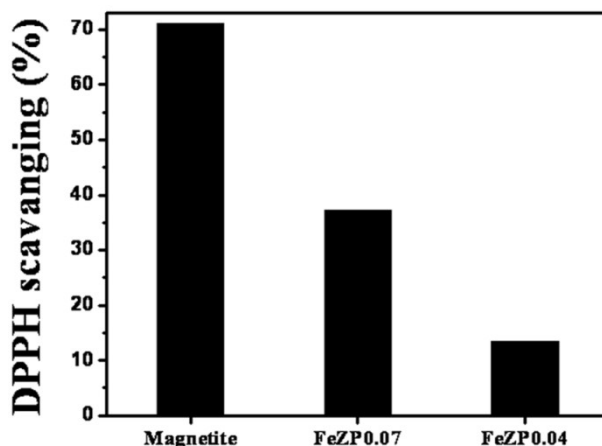
36 **Fig. S1** Quantitative measurement of ROS in MDA-MB-231 cells after 24 h of treatment with  
37 the nanoparticles.

39 **2. DPPH radical scavenging analysis**

40 The generation of ROS from the nanoparticles (i.e. magnetite, FeZP0.07, and FeZP0.04)  
 41 was further ascertained from their DPPH (2,2-diphenyl-1-picrylhydrazyl) radical scavenging  
 42 activity. The purple colored DPPH molecule contains a stable free radical that changes to a  
 43 yellow colored stable compound upon reaction with a ROS. The decaying of purple coloration of  
 44 the DPPH solution, that can be monitored spectrophotometrically at 517 nm thus, will give a  
 45 measure of the ROS produced by the nanoparticles. For the study, 10 mg nanoparticles were  
 46 added to 2 mL of 20  $\mu$ M DPPH solution in ethanol and agitated for 30 min in absence of light.  
 47 Subsequently, the absorbance of the supernants was measured at 517 nm and the scavenging  
 48 percentage of the samples were calculated using the following formula:

49 DPPH scavenging (%) =  $(A_C - A_S / A_C) \times 100$

50 where,  $A_C$  is the absorbance of blank DPPH and  $A_S$  is the absorbance of DPPH solution in  
 51 presence of nanoparticles. The results depicted in Fig. S2 revealed that MNPs exhibit DPPH  
 52 radical scavenging of 71.1%, whereas the scavenging was observed to be 36.2 and 13.3% in  
 53 FeZP0.07 and FeZP0.04 respectively. The decrease in DPPH scavenging from MNPs to  
 54 FeZP0.04 indicated a significant reduction in ROS generation with increase in the thickness of  
 55 zirconium phosphate shell on magnetite core.

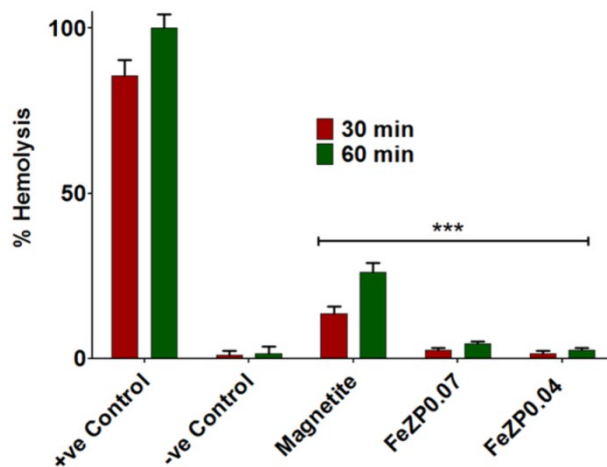


57 **Fig. S2** DPPH radical scavenging percentage of the nanoparticles.

59 **3. Hemocompatibility assay**

60 Hemocompatibility and hemolysis are major attributes for assessment of therapeutic  
 61 intervention of nanoparticles in drug delivery application, where nanoparticles with hemolysis of

62 5% or less are considered as non toxic and biocompatible<sup>1</sup> in therapeutic perspective. The  
 63 hemocompatibility of the prepared nanoparticles (i.e. magnetite, FeZP0.07, and FeZP0.04) was  
 64 ascertained from their hemocompatibility assay. The red blood cells (RBC) were collected from  
 65 the blood of BALB/c male mice (6 weeks older) by centrifugation using a ficoll density gradient.  
 66 For the assay, the collected RBC pellets were diluted in PBS (5% v/v) and then added to PBS (-  
 67 ve control), 1% Triton X-100 (+ve control) and the nanoparticles (suspended in 1X PBS), which  
 68 were then incubated at 37 °C for 30 and 60 min. The suspensions were centrifuged and the  
 69 absorbance of the supernatants was measured at 570 nm. The results of hemolytic assay (shown  
 70 in Fig. S3) revealed 15 and 23% hemolysis by MNPs after 30 and 60 min respectively. On the  
 71 contrary, insignificant percent of hemolysis (less than 5%) was observed in FeZP0.07 and  
 72 FeZP0.04 treatments even after extended exposure till 60 min, where the hemolysis was lowest  
 73 for the FeZP0.04 nanoparticles. Hemolytic assay of the nanoparticles indicates that the FeZP0.04  
 74 nanoparticles are hemocompatible and suitable for potential usage in biomedical fields.



75  
 76 **Fig. S3** Hemolytic assay of magnetite, FeZP0.07, and FeZP0.04 nanoparticles, where PBS and  
 77 1% Triton X-100 was taken as Negative and Positive controls respectively.  
 78 Each bar indicate the means  $\pm$  SD ( $n = 3$ ) with  $P < 0.001$ .  
 79

80 **4. References**

81 1 M. He, Z. Zhao, L. Yin, C. Tang and C. Yin, *Int. J. Pharm.*, 2009, **373**, 165-173.